# REHABILITATION OF COMPOSITE STEEL BRIDGES USING GFRP PLATES

A.A. El Damatty [1], M. Abushagur [2], M.A. Youssef [3]

[1] Associate Professor, [3] Assistant Professor
*Department of Civil and Environmental Engineering, The University of Western Ontario, London, ON, CANADA, N6A 5B9*
[1] Tel.: 1-519-661-2111 Ext. 88203, Fax: 1-519-661-3779, E-mail: damatty@uwo.ca

[2] *Assistant Professor, Department of Civil Engineering, University of El-Fatah, Tripoli, Libya*

## Abstract

The current study is a part of an extensive research program conducted to assess the use of Glass Fibre Reinforced Plastic (GFRP) sheets in enhancing the flexural capacity of steel beams. The properties of a heavy-duty adhesive system that can be used to bond GFRP sheets to the flanges of steel beams were experimentally determined in a previous study. The excellent performance of a W-shaped steel beam strengthened using GFRP sheets has encouraged the authors to assess the applicability of this technique to composite steel bridges.

The dimensions and cross section properties of a real composite steel plate girder bridge are considered in a case study analysis. A detailed nonlinear numerical model is developed for the bridge before and after attaching GFRP sheets to the bottom flange of its steel girders. Nonlinear moving load analyses are first conducted to determine the critical truck locations that will lead to maximum GFRP axial stresses, and maximum adhesive shear and peel stresses. Using these configurations, nonlinear analyses are then conducted to assess the increase in the bridge capacity that can be achieved by bonding 38 mm GFRP sheet to the bottom flange of its steel girders.

*Keywords*: Rehabilitation, Steel Girders; Glass Fibre Reinforced Plastic; Finite Element; Adhesive Failure, Bridge

## Introduction

In the last four decades, the American Association of State Highway and Transportation Officials (AASHTO) and the Federal Highway Administration (FHWA) have established programs to rate bridges through biannual evaluations. The data collected show that more than one third of the highway bridges in the United States are graded substandard. In Canada, the state of bridges is suspected to be more severe due to the harsh weather conditions. The continuous use of deicing salts on highways in winter would inflict higher damage on the bridge infrastructure. Figure 1 published by the National Bridge Inventory (NBI) [1] indicates 167,566 deficient structures within the US highway bridge network. This represents 28% of the total inventory of highway bridges. One-third of these bridges have steel as the main carrying structural element. According to the NBI report, steel bridges are among the most recommended group for rehabilitation. Their problems include the need for upgrading to carry larger loads and more traffic. Accordingly, a cost-effective rehabilitation technique with minimum disruption is needed.

The current study is part of an extensive research program that investigates the use of Glass Fibre Reinforced Polymer (GFRP) sheets to rehabilitate steel structures in general and steel bridges in particular. In the first phase of this research project, El Damatty and Abushagur [2] investigated different types of adhesives that can be reliably used to bond the GFRP sheets to the steel sections. Based on an extensive experimental study, they proposed the use of a methacrylate adhesive system for such an application. In the same study and using an experimental-analytical approach, they determined the shear and peel stiffnesses and strengths of this type of adhesive.

In a further study, El Damatty et al. [3] conducted flexural tests of W-shaped steel beams strengthened using GFRP sheets. In these tests, 19 mm GFRP sheets were bonded to the top and bottom flanges of the steel beam using the methacrylate adhesive system. The test results

indicated that the addition of the GFRP sheets provided an increase of about 15%, 23%, and 78% in the initial stiffness, yield moment, and ultimate moment of the steel beam, respectively. The tests have indicated an excellent performance of the adhesive and have shown that failure of the rehabilitated beam occurred when the tensile stresses in the GFRP sheet reached their ultimate values.

Previous studies conducted by other researchers and related to the application of composite material in retrofitting steel structures focused mainly on the use of Carbon Fibre Reinforced Plastic (CFRP) sheets. Sen and Liby [4] tested six steel beams after bonding CFRP sheets to their bottom flange. A considerable increase in the capacity of composite beams was reported. Miller et al. [5] used CFRP plates to strengthen four steel bridge girders. The girders were strengthened by bonding the CFRP sheets to the bottom flange. The experimental results indicated that the stiffness of the rehabilitated girders increased by 10% to 37%. Mertz and Gillespie [6] tested eight steel beams that were retrofitted using CFRP sheets. The study showed an average of 25% increase in stiffness and 100% increase in the ultimate load carrying capacity. In a recent study by Tavakkolizadeh and Saadatmanesh [7], six composite beams consisting of a W355X13.6 steel section and a 75 mm thick by 910 mm wide concrete slab were tested under pure bending in a four-point load setup. Some of the specimens were damaged and some were left intact to investigate the efficiency of repair and rehabilitation, respectively. They reported that the CFRP sheets can significantly increase the ultimate load carrying capacity of the intact girders and restore the ultimate load carrying capacity and stiffness of damaged composite girders. Adhesive peel and shear failures were the predominant mode of failure in all above cases.

Although CFRP sheets have higher mechanical properties, especially elastic modulus, when compared to GFRP sheets, their application in retrofitting steel structures has the following drawbacks:

1) Due to the superior mechanical properties of the CFRP sheets, failure of the retrofitted steel beam generally occurs in the adhesive and thus the capacity of the CFRP sheets is not fully utilized.
2) Galvanization can occur when steel and carbon surfaces are in direct contact.
3) CFRP cost is much higher than GFRP.

In case of employing GFRP sheets, a larger thickness compared to typical CFRP sheets' thicknesses is needed to compensate for their lower stiffness. Previous analytical and experimental studies conducted by the authors indicated that the full capacity of the GFRP sheet can be reached while the shear and peel stresses in the adhesive are less than their ultimate values. This reflects an efficient use of GFRP sheets in retrofitting steel beams. Additionally, galvanization is not a problem when GFRP sheets are bonded to steel. GFRP sheets are also easy to handle due to their lightweight, easy to apply through bonding to the steel using heavy duty adhesive, and create a corrosion protective layer for the steel.

In the current study, the research efforts in the composite application of steel and GFRP are extended by assessing the use of GFRP sheets in upgrading the load carrying capacity of a composite steel/concrete plate girder bridge. The paper starts by describing the dimensions and properties of the bridge used as a case study in this investigation. The bridge is designed to satisfy the serviceability and strength limit state design conditions using the loads specified by the Canadian Highway Bridge Design Code (CHBDC) [8]. The cross section dimensions are carefully selected such that no reserve in strength exists under the factored loads specified in the

CHBDC. Accordingly, the bridge would become unsafe in case of increase in the specified live load values. The objective of the study is to assess if the addition of GFRP sheets can increase the strength of the bridge to be able to accommodate a 25% increase in live loads. The study is conducted numerically using a nonlinear finite element model. Nonlinear moving load analysis is conducted to determine the critical truck position for various components of the strengthened bridge. Various possible modes of failure are considered to judge on the increase in the load capacity using three different lengths of the GFRP sheet.

**Bridge Description**

The considered bridge is composed of a 240 mm cast-in-place concrete slab supported by five simply supported built-up steel girders spanning 24.85 m. Details of the bridge cross section are provided in Figure 2. The girders height, web thickness, flange width, and flange thickness are 910 mm, 12 mm, 307 mm, and 20 mm, respectively.

The shear connectors consist of two rows of studs connecting the top flange of each girder and the concrete slab. The diameter and height of the shear studs are 20 mm, and 100 mm, respectively. The transverse distance between the studs is 209 mm and their longitudinal spacing is 356 mm for the middle 14.6 m of the girders and 280 mm for the rest of the girders.

**Bridge Loading**

The dead load acting on a unit length of an intermediate girder is estimated as 13.31 kN/m. According to the Canadian Highway Bridge Design Code [8], two cases of live load have to be considered in the design:

a. A truck having the profile shown in Figure 3.

b. 70% of the truck weight applied simultaneously with a uniformly distributed load of 9 kN/m.

Preliminary analysis indicates that the first load case is critical for the considered bridge.

**Retrofit Procedure**

The suggested retrofit procedure involves bonding GFRP sheets to the bottom flanges of of the steel girders. The considered GFRP sheets have a thickness of 19 mm, width of 307 mm matching the flange width, and a variable length to be estimated from the analysis as described later. Two layers of GFRP sheets are suggested for retrofitting the considered bridge; i.e. a total thickness of 38 mm for the GFRP material is applied. The proposed 19 mm GFRP sheets were used in the experimental program conducted by El Damatty and Abushagur [2] and El Damatty et al. [3]. They consist of a large number of unidirectional layers with few intermediate random layers providing the transverse resistance needed during handling and shipping. The tensile strength of the GFRP layer as evaluated experimentally by El Damatty et al. [3] is equal to 206.85 MPa. Similarly, the modulus of elasticity of the GFRP sheets is $1.72 \times 10^4$ MPa.

Based on the test results reported by El Damatty and Abushagur [2], a methacrylate adhesive system (A0420) is suggested for such an application involving bonding plastic and steel surfaces. According to the manufacturer, the optimum thickness of the adhesive is 0.79 mm. the stiffness of the adhesive was simulated by El Damaty and Abushagur [2] using spring systems representing the shear and peel behaviour of the adhesive. The lower limits resulting from the testing program conducted by El Damatty and Abushagur [2] were used to define the ultimate strength of adhesive. These correspond to an adhesive shear strength of 21.79 MPa and adhesive

peel strength of 4.0 N/mm. Step by step procedure for bonding the GFRP sheets is described in details by El Damatty et al. [3].

**Finite Element Modeling**

A detailed finite element modeling is developed for an intermediate girder. The model includes the portion of the concrete slab contributing to the rigidity of the intermediate girder. The modeling is conducted using the finite element program ANSYS [9].

Frame elements with shear deformations included are used to model separately each part of the cross section: steel girder, concrete slab and GFRP sheets. A sketch of the finite element model is provided in Figure 4. In this figure, the centerline of the steel girder is modeled using a number of frame elements. Vertical rigid arms coinciding with the location of the shear studs are attached above and below the frame elements. The length of each rigid arm is equal to half the depth of the girder. Similarly, the centerline of the concrete slab and the GFRP sheets are simulated using frame element with rigid arms attached having a length that is equal to half the thickness of these layers. Due to presence of shear studs, rigid connections are assumed at the intersection between the rigid arms of the steel girder and the concrete slab. The adhesive shear and peel springs constants, previously evaluated by El Damatty and Abushagur [2], are multiplied by the tributary area of each rigid arm leading to the stiffness value of the intermediate linear springs attached between the steel and the GFRP sheets. A linear elastic behaviour was assumed for the frame elements simulating the GFRP sheets as well as those simulating the rigid arms.

A bilinear stress-strain curve, Figure 5, is used to describe the material behaviour of steel. The steel yield strength, $\sigma_y$, and its modulus of elasticity, $E_s$, are 300 MPa, and $2x10^5$ MPa, respectively. Its tangent modulus is assumed as 3% of its Elastic Modulus.

The material model of concrete in compression is described using the stress-strain curve shown in Figure 6. In this model, the concrete stress is assumed varying parabolically with its strain until reaching a strain value of 0.002. For values of strains above 0.002, the concrete stress remains constant at $f_c$' until reaching the failure strain, defined as 0.003. The concrete compressive strength, $f_c$', is 30 MPa .

**Moving Load Analysis**

The purpose of this set of analysis is to determine the position of the truck that leads to critical conditions of the retrofitted structure. A large number of nonlinear analyses are conducted by gradually moving the position of the truck along the length of the bridge. Each nonlinear analysis is conducted by applying a load combination (P) defined as follows

P = 1.1x Dead Load + 1.7 x ($\gamma$) x Truck Weight.

Where the load factors 1.7 and 1.1 are as specified in the CHBDC, [8], $\gamma$ is a magnification analysis factor that is gradually increased from zero to a value 1.25.

For each nonlinear analysis, representing a specific location of the truck, the distributions of the following functions are plotted along the length of the girder:

a. Axial strains at the top surface of the concrete slabs.

b. Axial stresses at the bottom surface of the GFRP sheet.

c. Shear stresses in the adhesive.

d. Peel stresses in the adhesive.

e. Shear forces in the shear studs.

The envelope diagrams for each one of these functions are obtained by repeating the analysis while gradually moving the position of the truck.

These envelope diagrams are then used to identify the critical location corresponding to each one of these functions as well as the truck position leading to an absolute maximum value at this critical location. This set of analysis is conducted for the steel girder retrofitted using a GFRP overlay having a length of 18 m.

**Analysis to Identify Failure Load**

This set of analysis is conducted on the initial un-retrofitted configuration of the bridge together with three retrofitted cases using three values for the length of the GFRP sheets: [a] 15 m (R-15), [b] 18 m (R-18), and [c] 20 m (R-20).

For each case, a number of nonlinear analyses is conducted using the critical truck position established from the previous set of analyses. Each nonlinear analysis is conducted by applying a load combination (P) as defined above.

The nonlinear analyses are conducted by applying the dead load first and then gradually increasing the applied live load using the factor $\gamma$. The following failure modes can govern the load carrying capacity of the retrofitted bridge:

1 Concrete crushing: concrete strain reaches its ultimate value of 0.003.

2 GFRP sheet tensile failure: GFRP tensile stress reaches its ultimate strength value of 206.85 MPa.

3 Adhesive shear failure: adhesive shear stress reaches its ultimate value of 21.79 MPa. This value is based on the lower limit of the test results reported be El Damatty and Abushagur [2].

4 Adhesive peel failure: adhesive peel stress reaches its ultimate value of 4 N/mm. This value is also based on the lower limit of the test results reported by El Damatty and Abushagur [2].

5 Failure of the shear studs: the shear force in the studs reaches its ultimate capacity of 97.1kN. This value is calculated according to CHBDC [8] and the Canadian Steel Code [10].

**Moving Load Analyses Results**

The envelope diagrams obtained from the moving analyses are presented at $\gamma$ value of 0.5 and 1.25, respectively. For $\gamma = 0.5$, steel stresses are within the linear range of the material's behaviour. While for $\gamma = 1.25$, steel stresses exceed its yield value. The envelope diagrams for various functions resulting from these analyses are discussed in this section.

The envelope diagrams for the axial compressive strains developing at the top fibres of the concrete slab are presented in Figure 7 for the two analysis factors. The shape of these diagrams resembles the envelope diagram for bending moment along the length of the girder. The absolute maximum strain occurs at the center of the girder and corresponds to a truck position in which the 175 kN load is located 1.1 m from the centerline of the girder. At this location, the centerline of the girder is located midway between the center of gravity of the truck and the heaviest truck wheel. This critical truck position will be referred to as "TL1". In the same figure, the envelope diagram for the axial strains developing at the top of the concrete slab of the original bridge is provided. It is noticeable that at $\gamma = 1.0$ , i.e. for the factored load that is currently specified in the code, the strains reach a value of 0.003 at mid point of the bridge. This strain value corresponds

to the ultimate capacity of concrete. As such, the un-retrofitted bridge cannot sustain an extra increase in the design live load values.

The envelope diagrams for the axial stresses developing at the bottom layer of the GFRP sheets are provided in Figure 8. Similar to strains in concrete, the absolute maximum stress occurs at the center of the girder and results from the truck position “TL1”.

The envelope diagram for the shear stresses developing in the adhesive is plotted in Figure 9. In this case, the absolute maximum shear occurs at the edge of the GFRP sheet. This absolute maximum value occurs when the heaviest end wheel load coincided with the edge of the GFRP sheet. This truck configuration will be referred to as “TL2”.

The envelope diagram for the adhesive peel stresses (force/unit area) is given in Figure 10. In this figure, the negative values shown at the edge of the GFRP represent a state of separation between the steel girder and the GFRP sheet. The peel strength, obtained through a standard ASTM D1878 test, is presented as force per unit length. The corresponding acting peel force can be obtained by integrating the peel stresses within the length at which separation tends to occur. This integration is conducted for all considered truck positions. The maximum peel force is found to be equal to 1.75 N/mm and to correspond to truck configuration “TL1”.

The envelope values for the shear forces developing in the studs are shown in the bar charts provided in Figure 11. The absolute maximum force occurs at the stud that is closer to the support of the girder. The truck configuration “TL3” corresponding to this critical value corresponds to allocating the heaviest end truck wheel just before the edge stud.

Results obtained from this set of analysis indicate that three truck configurations should be considered in the analysis and design of a composite simply supported steel girder retrofitted using GFRP sheets. These can be described as follows:

a. Configuration “TL1”, at which the centerline of the girder is located midway between the center of gravity of the truck and the heaviest truck wheel that leads to critical values for the axial stresses in the GFRP and the concrete slab as well as maximum peel forces in the adhesive.
b. Configuration “TL2”, at which the heaviest end wheel is located at the edge of the GFRP sheet that leads to maximum shear stresses in the adhesive.
c. Configuration “TL3”, at which the heaviest end wheel load is located at the edge stud that leads to maximum shear forces in the shear studs.

**Results from Analyses to Identify Failure Load**

The three retrofitted cases (R-15), (R-18) and (R-20) of the girders are analyzed using the three truck configurations “TL1” “TL2” and “TL3”. The analyses include the effect of factored dead load as described in the previous section. In addition, the Un-Retrofitted (UR) girder is analyzed under load configuration “TL1” to determine its ultimate carrying capacity that is expected to be governed by concrete crushing. The relationship between the axial strain, developing at mid-span of the concrete slab, and the load factor “γ”, resulting from the analysis of the (UR), (R-15), (R-18), and (R-20) cases, under load configuration “TL1” is provided in Figure 12. Assuming that the ultimate compressive strain value for concrete is 0.003, it can be seen that the load carrying capacity of the un-retrofitted bridge corresponds to γ=1. This implies that the bridge with its current configuration cannot sustain any increase in the specified truck weight. Meanwhile, for the three retrofitting schemes, the load factor “γ” can reach a value of 1.3 before the concrete slab reaches its ultimate capacity. The graph also indicates that the length of the GFRP sheets has almost no effect on the reduction in the stresses in the concrete slab. The relationship between

the axial tensile stress at mid-span of the GFRP layer and the load factor "γ" for the three retrofitting schemes resulting from nonlinear analyses under load configuration "TL1" is provided in Figure 13. Here, the length of the GFRP has some effect on the induced axial stresses. Assuming an ultimate strength capacity of 206.85 MPa for the GFRP sheets, it can be seen that both the (R-18), and (R-20) schemes achieve the same load factor capacity of $\gamma = 1.25$. Results indicate that**,** as far as axial stresses in the GFRP are concerned, 18 meters is the optimum length for the sheets.

The relationship between the absolute shear stress in the adhesive and the load factor "γ", shown in Figure 14, result from the analysis using the truck configuration "TL2". The figure indicates that, using an ultimate shear strength value of 21.79 MPa, both the (R-18), and (R-20) cases achieve a load factor $\gamma = 1.25$.

Finally, the absolute values of the peel separating force (per unit length) resulting from analyses using the load configuration 'TL1" are plotted versus the load factor "γ" in Figure 15. Based on ultimate strength value of 4.0 N/mm, it can be seen that the (R-18), and (R-20) cases achieve the load factor of $\gamma = 1.25$.

Generally based on the results of all these analyses, it can be stated that bonding two 19 mm thick GFRP sheets having each a length of 18 m to the bottom face of the steel girders achieves an increase of 25% in the truck weight carrying capacity of the bridge.

## Conclusions

The current study assesses the applicability of using GFRP sheets as means to strengthen existing composite steel bridges. The concept involves bonding GFRP plates to the bottom flanges of the steel girders using a heavy-duty adhesive system. A detailed nonlinear finite element modeling,

that incorporates adhesive properties based on previously conducted test results, is conducted in this study. Moving load analysis is conducted first to determine the critical load configuration corresponding to the absolute maximum of various parameters that may govern the failure of the retrofitted girders.

The analyses reveal that the same load configuration that leads to maximum bending moment is critical for concrete, GFRP, and adhesive peel stresses. The absolute maximum adhesive shear stress value is governed by another load configuration corresponding to maximum shear force at section located at the edge of the GFRP sheet. The study proceeds by conducting nonlinear analyses using three different values for the length of the GFRP sheets under the critical load configuration established from the moving load analysis. A 25% increase in the truck weight carrying capacity of the girders is achieved using this retrofitting scheme without suffering from premature failure in the concrete, GFRP or adhesive.

**References**

1. National Bridge Inventory, `Count of deficient highway bridges', Bridge Program Group, the Federal Highway Administration, Washington, D.C., 2002.
2. El Damatty, A. and Abushagur, M., `Testing and modeling of shear and peel behaviour for bonded steel/FRP connections', Journal of Thin Walled Structures.**41** (11), 2003, 987-1003.
3. El Damatty, A., Abushagur M. and Youssef, MA, `Experimental and Analytical Investigation of Steel Beams Rehabilitated Using GFRP Sheets', Journal of Steel & Composite Structures **3** (6), 2003, 421-438.

4. Sen, R. and Liby, L., `Repair of Steel Composite Bridge Sections Using Carbon Fiber Reinforced Plastic Laminates', Report FDOT-510616, Florida Department of Transportation, Tallahassee, FL, 1994.
5. Miller, T.C., Chajes, M.J., Mertz, D.R. and Hastings, J.N., `Strengthening of a Steel Bridge Girder Using CFRP Plates', ASCE, Journal of Bridge Engineering **6** (6), 2001, 512-522.
6. Mertz, D. and Gillespie, J., `Rehabilitation of steel bridge girders through the application of advanced composite material', Report NCHRP 93-ID11, Transportation Research Board, Washington, D.C., 1996, 1-20.
7. Tavakkolizadeh M. and Saadatmanesh H., `Strengthening of Steel-Concrete Composite Girders Using Carbon Fiber Reinforced Polymers Sheets`, Journal of Structural Engineering, 2003, 30-40.
8. CAN/CSA-S6-00, `Canadian highway bridge design code', Canadian Standards Association, Rexdale, Ontario, 2000.
9. ANSYS program, version 5.7, ANSYS Inc., Canonsburg, PA.
10. CSA-16-1-M89, `Handbook of Steel Construction', Canadian Institute of Steel Construction, Willowdale, Ontario, 1989.

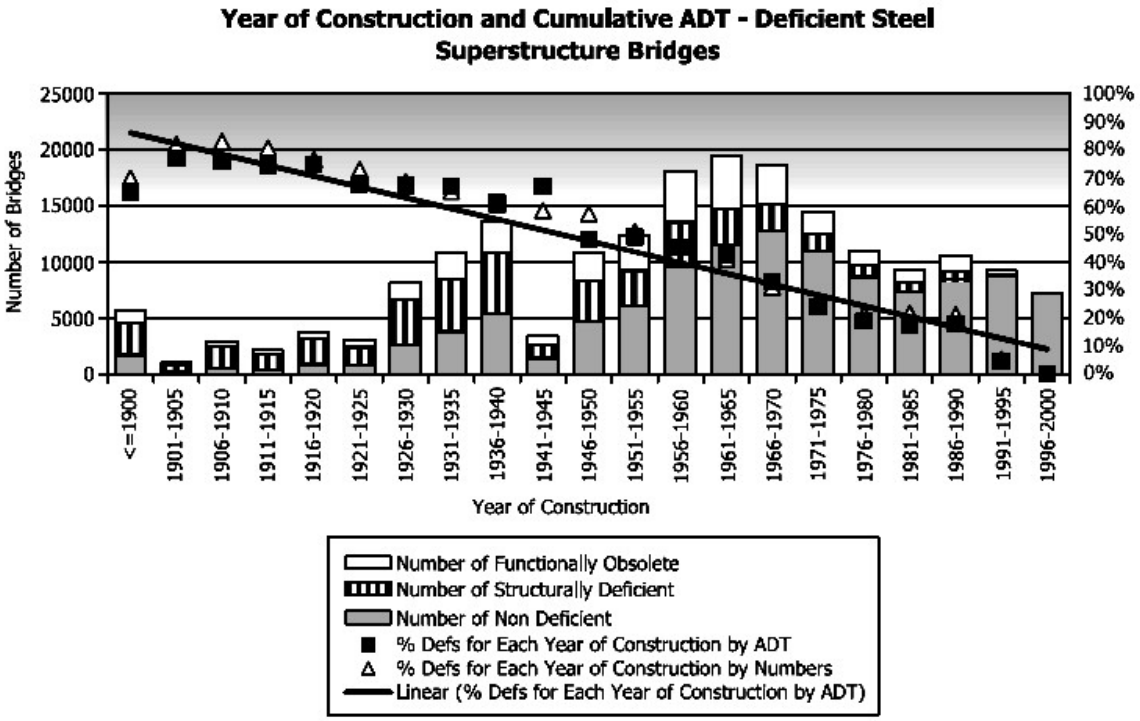


Figure 1 Highway Bridge Network in USA [1]

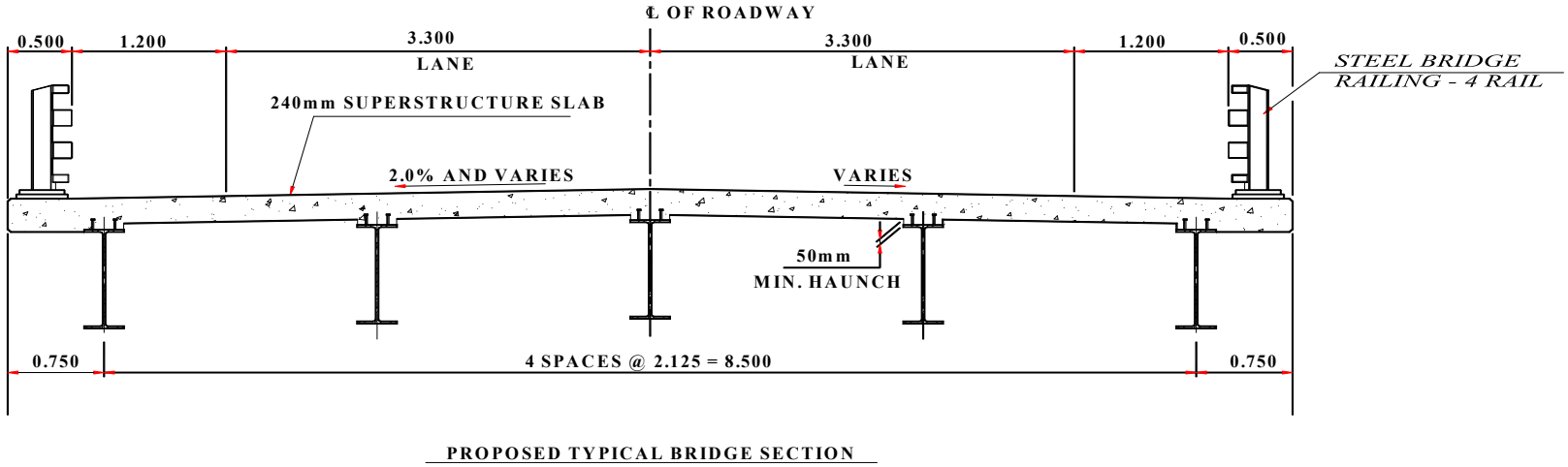


PROPOSED TYPICAL BRIDGE SECTION

Except otherwise stated, all dimension are in meters

Figure 2 Bridge Cross Section

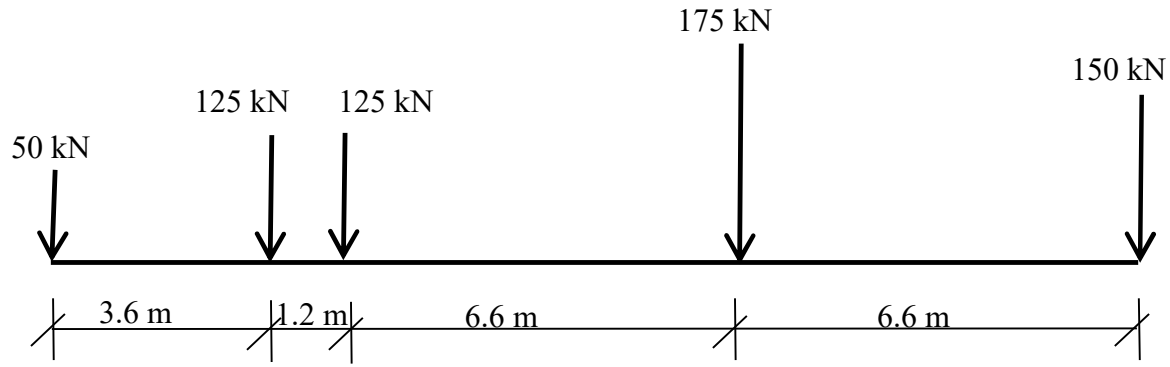


Figure 3 Truck Profile

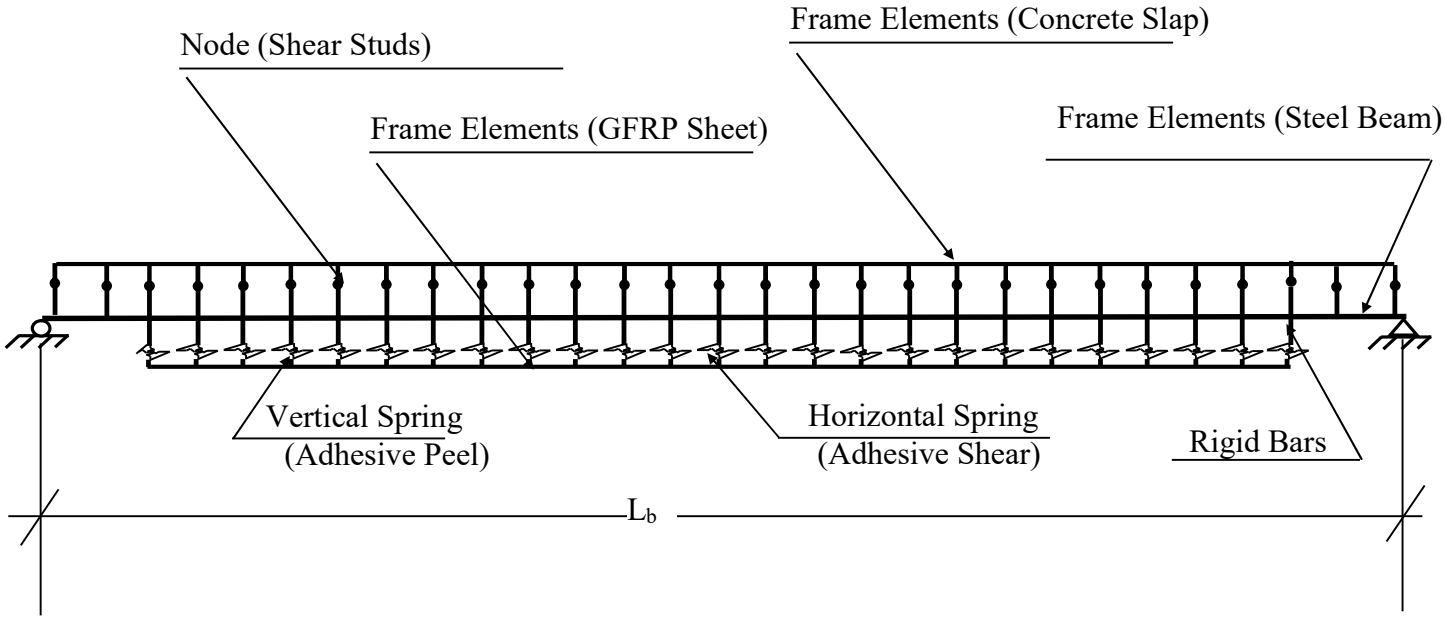


Figure 4 Typical Finite Element Model

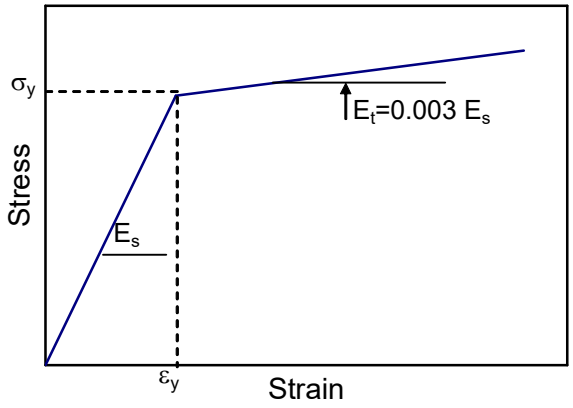


Figure 5 Steel Stress-Strain Diagram

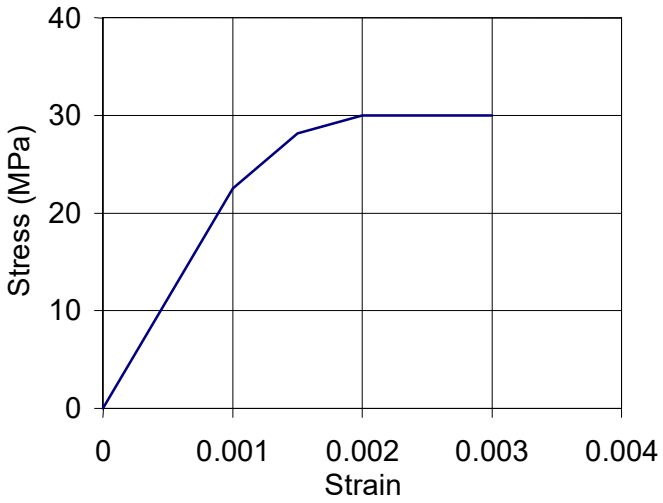


Figure 6 Concrete Stress-Strain Diagram

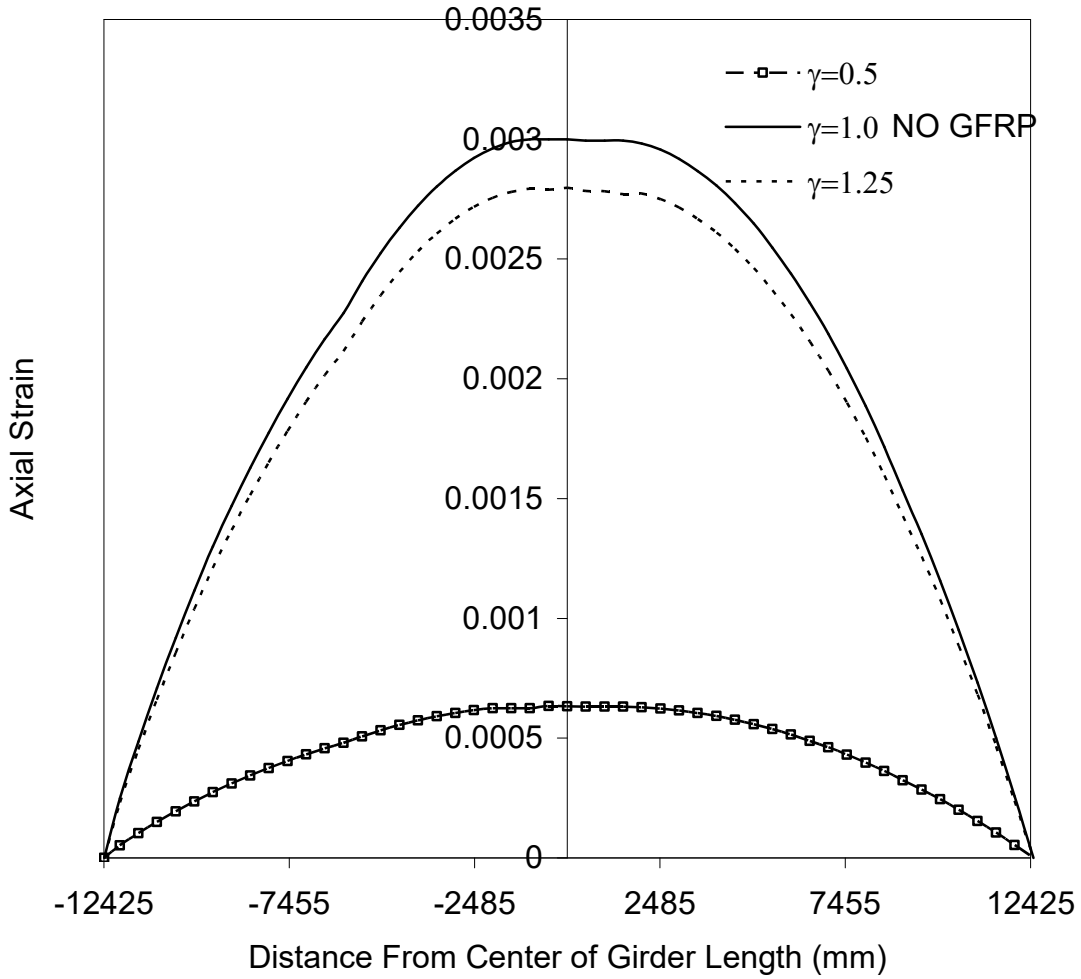


Figure 7 Envelope Diagram for Axial Strain in Concrete Slab.

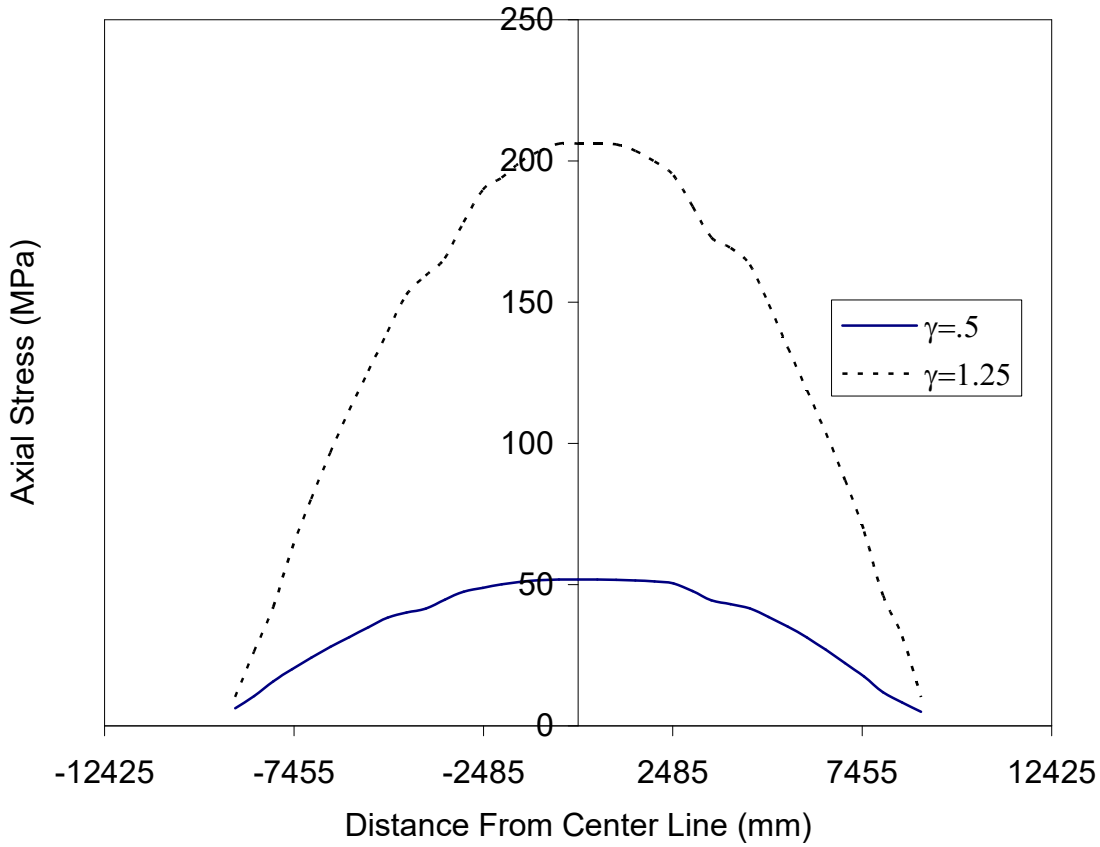


Figure 8 Envelope Diagram for Axial Stresses in GFRP Plates.

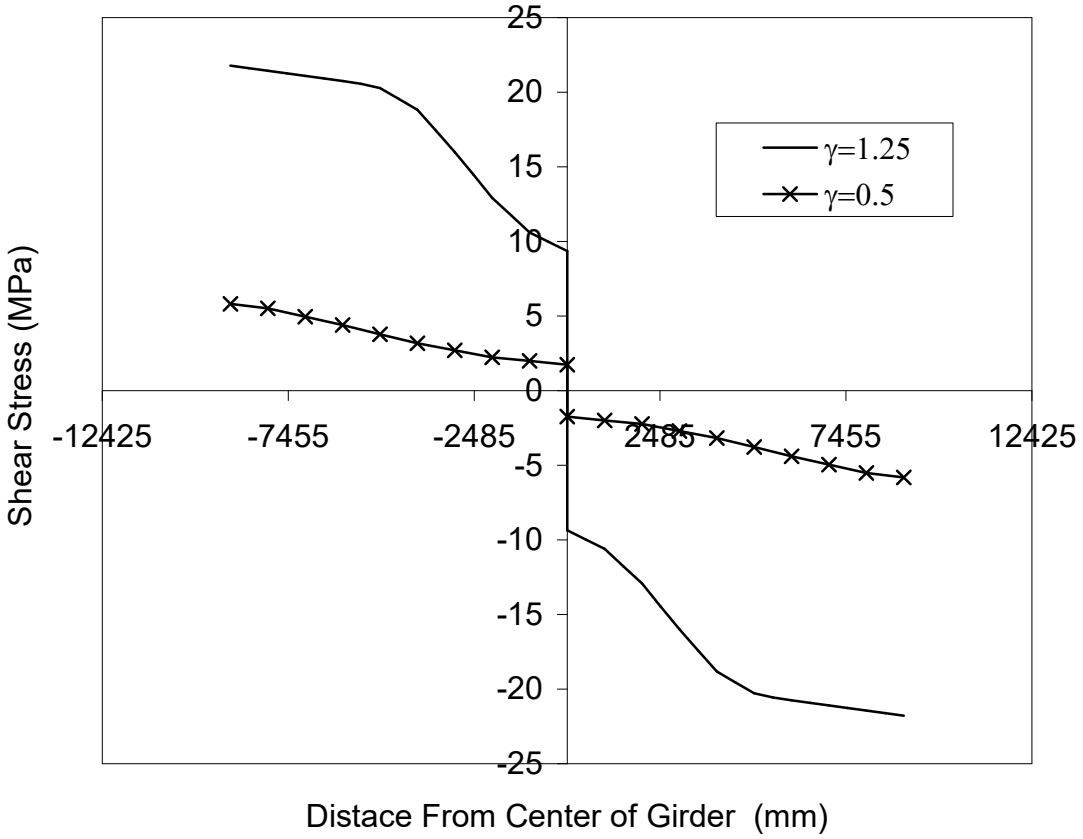


Figure 9 Envelope Diagrams for Shear Stress in the Adhesive.

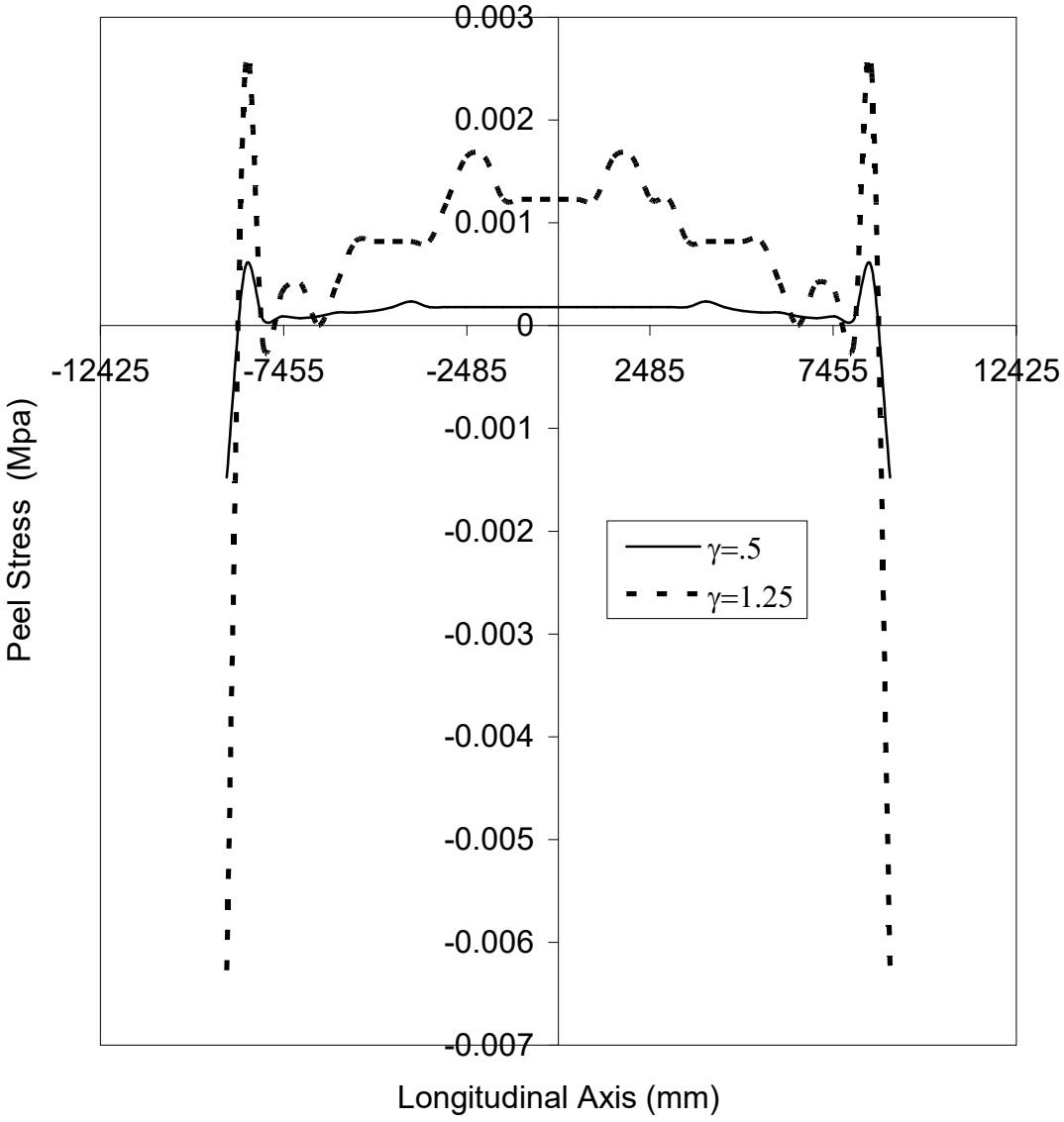


Figure 10 Envelope Diagram for Peel Stresses in Adhesive

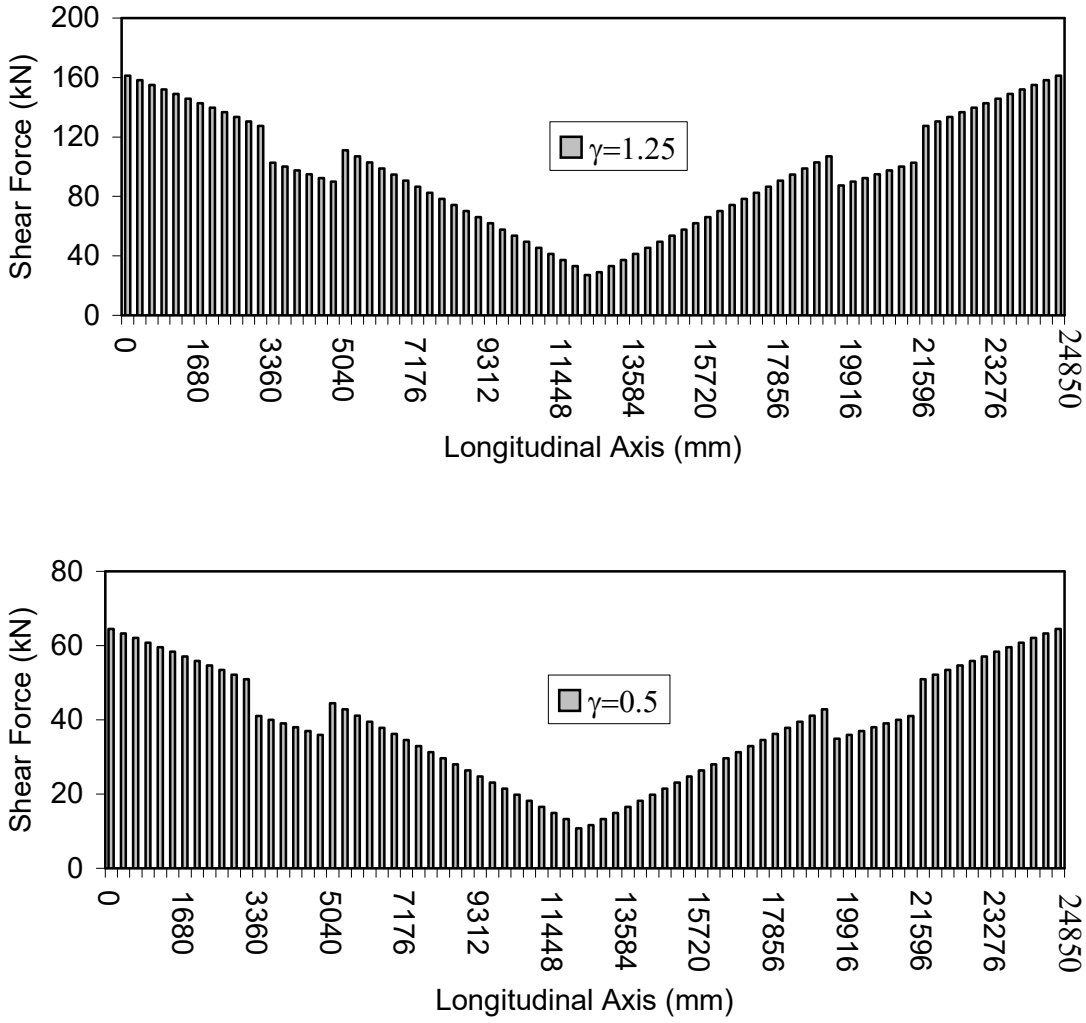


Figure 11 Envelope Bar Charts for Shear Studs.

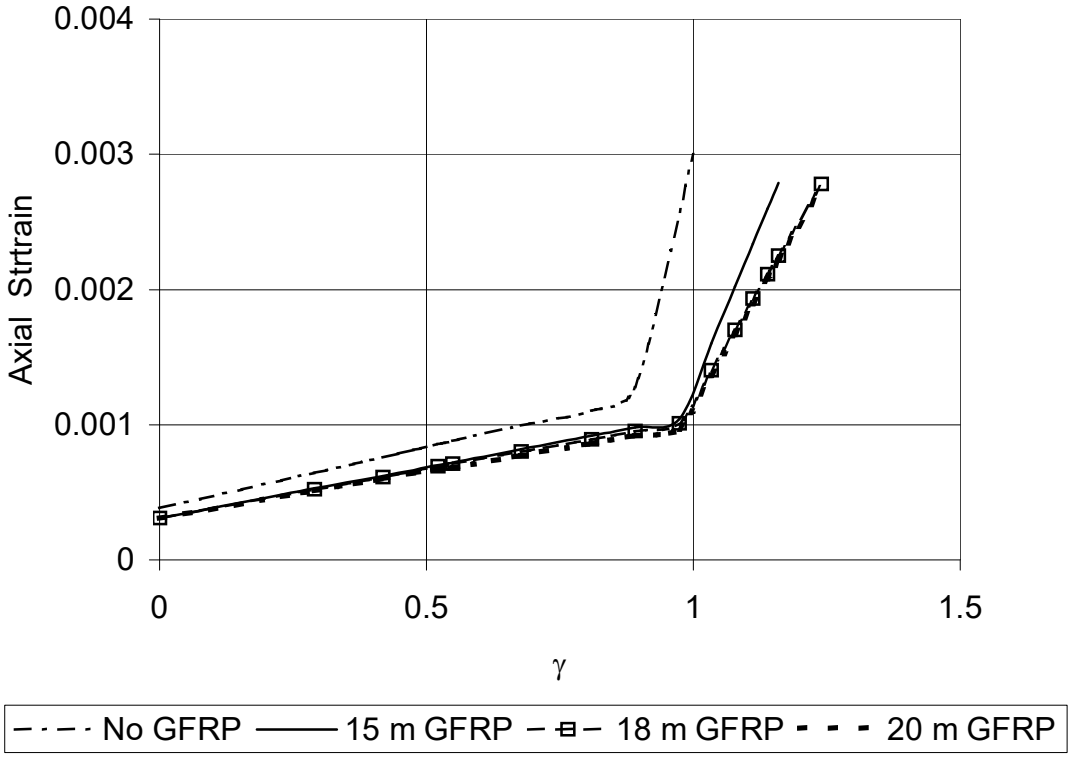


Figure 12 Variation of Axial Strain at Mid-Span of Concrete with Load Factor

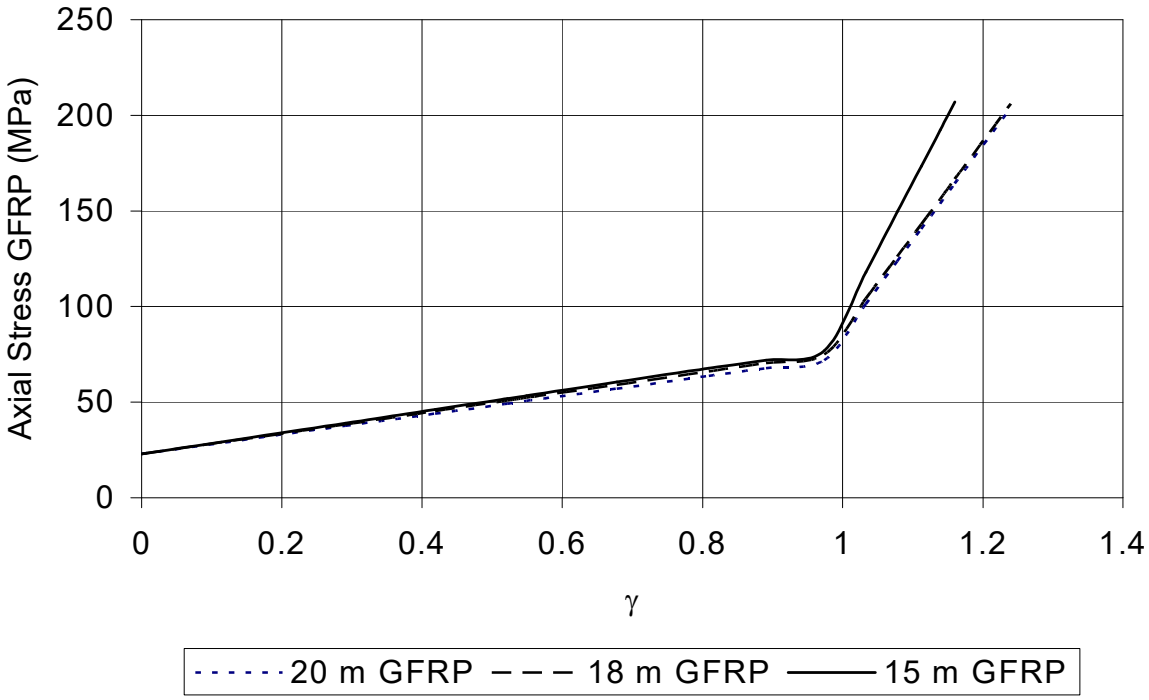


Figure 13 Variation of Axial Stress at Mid-Span of GFRP Layer with Load Factor γ

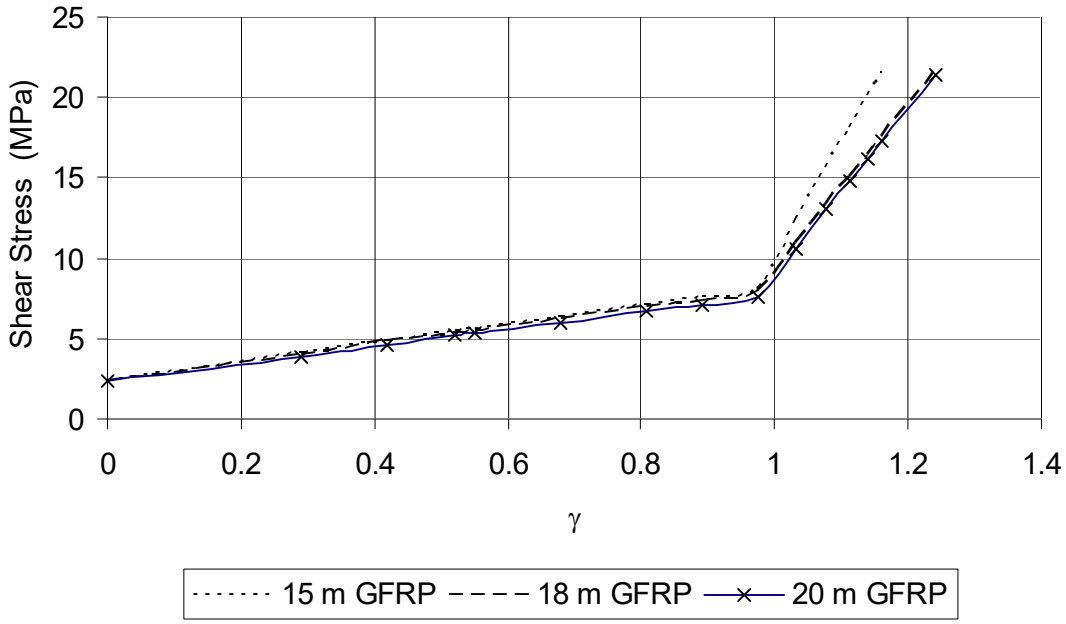


Figure 14 Variation of Absolute Shear Stress in Adhesive with Load Factor γ

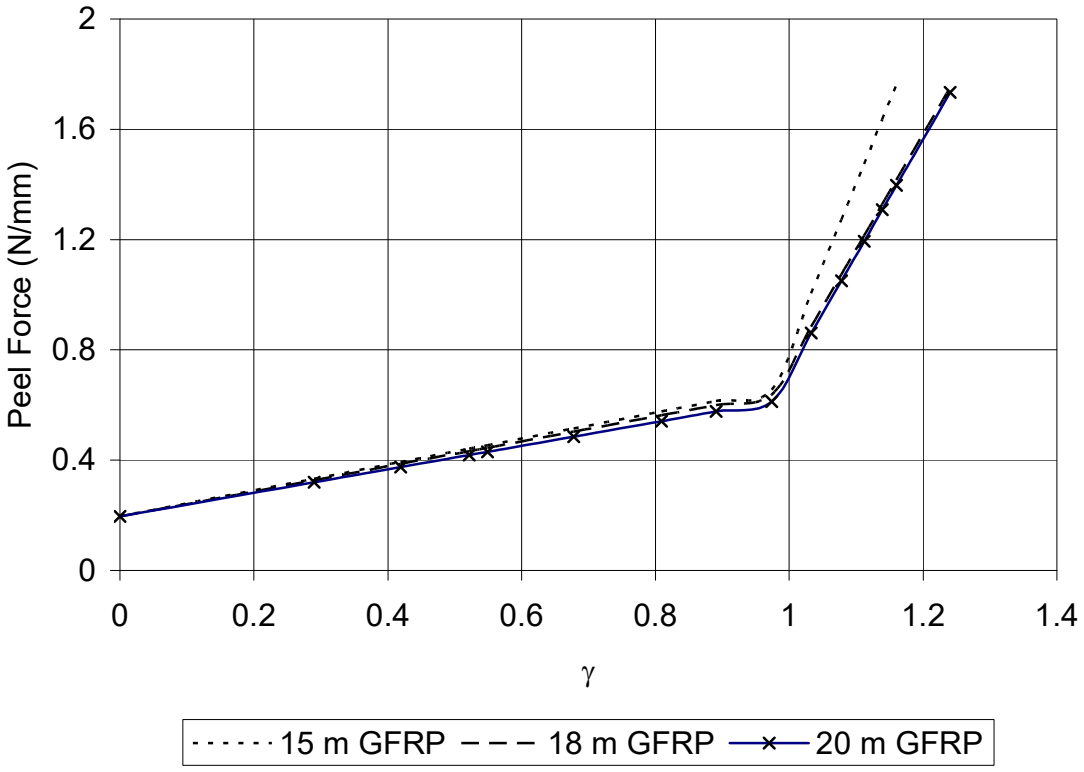


Figure 15 Variation of Absolute Peel Force in Adhesive with Load Factor γ